



A fully coupled thermo-hydro-mechanical model for unsaturated porous media

Weizhong Chen^{*}, Xianjun Tan, Hongdan Yu, Guojun Wu, Shanpo Jia

State Key Laboratory of Geomechanics and Geotechnical Engineering, Institute of Rock and Soil Mechanics, Chinese Academy of Sciences, Wuhan, 430071, China

Received 12 February 2009; received in revised form 13 September 2009; accepted 27 September 2009

Abstract: In examining potential host rocks for such purposes as the disposal of high-level radioactive wastes, it is important to understand the coupled thermo-hydro-mechanical (THM) behavior of a porous medium. A rigorous and fully unified coupled thermo-hydro-mechanical model for unsaturated porous media is required to simulate the complex coupling mechanisms involved. Based on modified Darcy's and Fourier's laws, equations of mechanical equilibrium, mass conservation and energy conservation are derived by introducing void ratio and volumetric liquid water content into the model. The newly derived model takes into account the effects of temperature on the dynamic viscosity of liquid water and void ratio, the influence of liquid flow on temperature gradient (thermo-osmosis), the influence on mass and heat conservation equations, and the influence of heat flow on water pressure gradient and thermal convection. The new coupled THM constitutive model is constructed by a finite element program and is used to simulate the coupled behavior of a tunnel during excavation, ventilation and concrete lining stages. Oil and gas engineering, underground disposal of nuclear waste and tunnel engineering may be benefited from the development of the new model.

Key words: porous media; unsaturated media; coupled thermo-hydro-mechanical (THM) model

1 Introduction

Coupled thermal-hydro-mechanical (THM) processes with multiphase flow are prevalent in a number of engineering applications. Some of the most important ones include nuclear waste disposal in geological media, deep underground injection of hazardous waste, geothermal energy extraction, enhanced recovery from oil and gas reservoirs, and underground storage of natural gas, etc..

Numerous studies have been conducted on both theoretical and experimental aspects of THM coupling. Following the basic framework of Biot, the first one to investigate poroelastic theory, many researchers have studied a variety of quasi-static and dynamic problems and analyzed the THM coupling behaviors of saturated media [1–3]. These studies were based on various constituents and small temperature assumptions, including incompressibility variations, thermal equilibrium of

solid and fluid phases, linear elastic behavior of solid phase, non-convective heat flow, absence of phase change of fluids, and constant material properties. Analytical solutions for thermoporoelastic models with constant material properties subjected to small perturbations about an initial state [4–9], and finite element solutions for thermoporoelasticity [10, 11] have been developed. These solutions are all based on conventional Darcy's and Fourier's laws for fluid flow and heat flow.

Earlier researches mentioned above have neglected the influence of temperature gradients on fluid flow (the thermo-osmosis effect, which is analogous to the Soret effect in solutions). Thermo-osmosis is an important coupling process defined in the thermodynamics of irreversible processes [11].

Porous media encountered in many engineering applications are unsaturated. Recent developments of unsaturated soils, both in laboratory experiments and numerical simulations, have been used successfully to describe flow processes in unsaturated porous media [12–14]. A commonly used approach for modeling water flow in unsaturated medium is the continuum approach. Armero et al. [15, 16] decomposed the fluid content into elastic and plastic portions, invoking an

extension of the Biot framework. Borja and Alarc [17] obtained a model based on mixture theory combined with the volume fraction concept. Diebels and Ehlers [18] developed a model considering the dynamic effect. A slightly different model by Wilmanski [19] and Kempa [20] introduced porosity into the balance equation.

Initiated in 1992, the DECOVALEX project is an international collaboration for advancing the understanding and modeling of coupled THM processes in geologic systems. The project has made important scientific achievements through four stages and is progressing in its fifth stage, which has played a key role in development of mathematical modeling of coupled THM and THMC (thermo-hydro-mechano-chemic) processes of geological media. A hydromechanical formulation for fractured rock, based on Boit's general effective stress theory, was developed by Noorishad et al. [21]. The coupled THM issues related to nuclear waste repository design and performance are reviewed [22]. Rutqvist et al. [23] presented a comprehensive analysis of governing equations for coupled THM processes in saturated and unsaturated geologic formulations as applied in the DECOVALEX project.

Although many mathematical models have been reported for porous media, the analyses using these models are often limited to simplifications such as non-deformable media, neglecting thermo-osmosis effects, or constant material properties. Most of these conditions are not justifiable for porous materials with very low hydraulic conductivity, high deformability and porosity.

In this paper, a fully coupled THM model is presented, which takes into account thermo-osmosis and deformation effects, nonlinear behavior including the effects of temperature on the dynamic viscosity of liquid water and the void ratio, the effects of liquid flow on the temperature gradient, and the effects of heat flow on water potential gradient.

2 Coupled THM model of unsaturated porous media

2.1 Basic assumptions

The coupled processes encountered in unsaturated media are complex. Transfer of heat, moisture and air in a deformable and unsaturated medium involves interaction of three different processes (thermal, mechanical, and fluid) and three different phases (solid, liquid, and gas). Water in the system may exist as liquid water or water vapor, and phase changes may occur due to variations in load and temperature. The

nature of this complex system makes it difficult to establish a general and complete mathematical model to include all possible coupled processes. Therefore, the following assumptions are introduced to simplify the modeling. (1) The density of solid grains is constant and the solid grains are incompressible, but the porous medium is deformable. (2) Deformations are small. (3) Liquid water and heat flow have two driving forces including water potential gradient and temperature gradient. (4) Water vapor is ignored. This means that the water flow does not undergo phase transformation, since the gas pressure is relatively large and the temperature variation is small for the problems studied at present. (5) Local thermal equilibrium exists between different phases. (6) The velocity of the solid skeleton is ignored.

2.2 Theoretical approach for unsaturated porous media

The water retention curve (increasingly known as the soil water characteristic curve) is important for unsaturated media because it represents the characteristics of an isothermal and volumetric equilibrium state. It assumes that water content is only a function of capillary pressure. However, it could vary with effective stress, as suggested by McDougall et al. [24]. In a non-isothermal situation, it is also temperature dependent due to the effect of trapped air and surface tension of the soil solution. So unsurprisingly, recent experimental evidence suggests that for non-isothermal deformable unsaturated media, the water retention curve needs to be modified to include temperature and stress effects [25].

For deformable media, void ratio changes with water potential, temperature and stress. Based on the concepts stated above, it is assumed that void ratio e and volumetric liquid water content n_l of unsaturated porous media are under the action of net mean stress σ , liquid water pressure p_l , air pressure p_a (positive for compressive pressure) and temperature T . Extending the isothermal model proposed by Wheeler and Sivakumar [26], the void ratio and volumetric liquid water content can be postulated as follows:

$$e = f_e(\sigma, p_c, T) \quad (1)$$

$$n_l = f_n(\sigma, p_c, T) \quad (2)$$

where the mean stress $\sigma = (\sigma_1 + \sigma_2 + \sigma_3)/3 + p_a$, and capillary pressure $p_c = p_l - p_a$.

The combination of $\sigma - p_a$ and p_c has been proved to be suitable for modeling the mechanical behavior of unsaturated soils from theoretical as well as experimental points of view [27]. This combination has the advantage of considering effects due to a change in the pore-water pressure. In addition, the

pore-air pressure is atmospheric for most practical engineering uses at the boundary.

According to Eq.(1), an increment of the void ratio, de , has a relationship with that of mean stress σ , capillary pressure p_c and temperature T , which can be expressed as

$$de = \frac{\partial e}{\partial \sigma} d\sigma + \frac{\partial e}{\partial p_c} dp_c + \frac{\partial e}{\partial T} dT \quad (3)$$

The increment of volumetric strain $d\varepsilon_v$ may be described as

$$d\varepsilon_v = \frac{de}{1+e} = \left(\frac{1}{1+e} \frac{\partial e}{\partial \sigma} \right) d\sigma + \left(\frac{1}{1+e} \frac{\partial e}{\partial p_c} \right) dp_c + \left(\frac{1}{1+e} \frac{\partial e}{\partial T} \right) dT = \frac{d\sigma}{K} + B_1 dp_c + B_2 dT \quad (4)$$

where K is the bulk modulus of the porous medium with respect to the change in net mean stress, B_1 is the coefficient of compressibility of the porous medium with respect to the change in capillary pressure, and B_2 is the thermal expansion coefficient.

Similarly, according to Eq.(2), the increment of volumetric liquid water content, dn_1 , can be expressed as

$$dn_1 = B_3 d\sigma + B_4 dp_c + B_5 dT \quad (5)$$

where B_3 , B_4 and B_5 are coefficients of water content changes due to changes in the net mean stress, capillary pressure and temperature, respectively.

Substitution of $d\sigma$ from Eq.(4) into Eq.(5) results in

$$dn_1 = B'_3 d\varepsilon_v + B'_4 dp_c + B'_5 dT \quad (6)$$

where $B'_3 = B_3 K$, $B'_4 = B_4 - B_1 B_3 K$, and $B'_5 = B_5 - B_2 B_3 K$.

2.3 Governing equations

For a fully coupled thermo-hydro-mechanical model of unsaturated porous media, four independent equations: (1) a mechanical equilibrium equation, (2) a water mass conservation equation, (3) an air mass conservation equation, and (4) an energy conservation equation are defined.

2.3.1 Mechanical equilibrium equation

The pore space of the porous medium is assumed to be occupied by liquid water and dry air. From Eq.(4), the elastoplastic constitutive relation of the incremental stress-strain relation can be obtained:

$$d\sigma_{ij} = C_{ijkl}^e (d\varepsilon_{kl} - d\varepsilon_{kl}^p) - KB_1 \delta_{ij} dp_c - \delta_{ij} dp_a - KB_2 \delta_{ij} dT \quad (7)$$

where C_{ijkl}^e is the classical elasticity matrix, ε_{kl} is the total strain tensor, and ε_{kl}^p is the plastic strain tensor.

Note that at full saturation $B_1 = 1/K$. KB_2 represents

the thermal expansion of the solid skeleton controlled only by the temperature of the solid constituent.

Assuming that the failure criterion for the porous medium follows the Drucker-Prager criterion, the yield surface f is given by

$$f = \alpha I_1 + \sqrt{J_2} - H = 0 \quad (8)$$

where I_1 is the first stress invariant, $I_1 = \delta_{ij} \sigma_{ij} = \sigma_{kk}$; J_2 is the equivalent deviatoric stress defined by the deviatoric stress component s_{ij} , $s_{ij} = \sigma_{ij} - \delta_{ij} \sigma_{kk} / 3$, $J_2 = s_{ij} s_{ij} / 2$; and α and H are material parameters which can be written as

$$\alpha = \frac{2 \sin \varphi}{\sqrt{3}(3 - \sin \varphi)} \quad (9)$$

$$H = \frac{6c \cos \varphi}{\sqrt{3}(3 - \sin \varphi)} \quad (10)$$

where c and φ are the cohesion and friction angle of the medium, respectively.

The mechanical equilibrium equation of the porous medium is given by

$$\sigma_{ij,j} + b_i = 0 \quad (11)$$

where b_i denotes the body force in the i th coordinate direction.

The relationship between the strain and displacement is given by

$$d\varepsilon_{ij} = \frac{1}{2} \left(\frac{\partial (du_i)}{\partial x_j} + \frac{\partial (du_j)}{\partial x_i} \right) \quad (12)$$

where u_i represents the displacement components of the solid skeleton.

Substitution of Eqs.(7) and (12) into Eq.(11) results in

$$\nabla^2 u_i + \frac{G}{1-2\nu} u_{j,ji} - p_{a,i} - KB_1 p_{c,i} - KB_2 T_{,i} + b_i = 0 \quad (13)$$

where ν is Poisson's ratio.

2.3.2 Water mass conservation equations

The most common method of modeling liquid flow in unsaturated media is to combine the equation of linear momentum balance for the liquid phase with the mass balance equation of the fluid. Neglecting the inertial and viscous effects, the equation of linear momentum balance for the water can be written as

$$\nu_{li} = - \frac{k_{lij}}{\mu_l} \left(\frac{\partial p_l}{\partial x_j} + \rho_l g_j \right) - k_{lTij} \frac{\partial T}{\partial x_j} \quad (14)$$

where k_{lTij} is the tensor of thermal coupling for water, ν_{li} is the water flow velocity, ρ_l is the water density, g_j is the j th component of gravitational acceleration vector in the j th direction, and k_{lij} is permeability tensor of water that can be determined directly in laboratory tests or indirectly by using the concept of

relative permeability of porous media to flow in water. k_{lij} is often written as

$$k_{lij} = k_{ij} k_1^r \quad (15)$$

where k_{ij} is the intrinsic permeability tensor of the porous medium, and k_1^r is the relative permeability of water.

The dynamic viscosity of water, μ_1 , is a function of the temperature [28], and

$$\mu_1 = 661.2(T - 229)^{-1.562} \times 10^{-3} \quad (16)$$

The second item in Eq.(14) represents the liquid water flow due to thermal gradients. Groenevelt and Kay [28] identified a corresponding physical mechanism that causes liquid and heat transport due to the heat of wetting of tightly bound water. This effect has been neglected in some previous mathematical models for deformable unsaturated media; Carnahan showed that the water flux due to a temperature gradient (identified as thermo-osmosis in the literature) can easily exceed the classical Darcy flux in low hydraulic conductivity media subjected to temperature gradients.

Based on Euler's rule, a representative unit body of volume Ω in a porous medium is chosen. Its external surface area is A with an exterior normal direction \hat{n} . The flow velocity through a differential surface element dA is \mathbf{v}_{li} , and the quantity of water that flows in a unit time through surface element dA is $\rho_1 \mathbf{v}_{li} \hat{n} dA$. Therefore, the total quantity through the total external surface area A is

$$T_A = \oint_A \rho_1 \mathbf{v}_{li} \hat{n} dA \quad (17)$$

A differential volume element $d\Omega$ is chosen in Ω . Because of this, the density and void ratio may change with time. Therefore, the rate of the water content increment in Ω is

$$T_{rw} = \int_{\Omega} \frac{\partial[\rho_1(1+e)n_1]}{(1+e)\partial t} d\Omega \quad (18)$$

If there is a source (or sink) within Ω , with an intensity q_1 , the additional water content intruded into (or extracted from) $d\Omega$, in unit time, is $\rho_1 q_1 d\Omega$. Then, the total water content that flows into or out of Ω in unit time, due to the presence of the source (or sink), is defined as

$$T_w = \int_{\Omega} \rho_1 q_1 d\Omega \quad (19)$$

According to the law of mass conservation, the increase in water content in Ω is equal to the amount produced by the source (or removed by the sink) minus the amount flowing out through the surface area, that is,

$$\int_{\Omega} \frac{\partial[\rho_1(1+e)n_1]}{(1+e)\partial t} d\Omega = \int_{\Omega} \rho_1 q_1 d\Omega - \oint_A \rho_1 \mathbf{v}_{li} \hat{n} dA \quad (20)$$

Equation (20) is the governing equation for water flow in Ω in an integral form based on the Gauss divergence theorem:

$$\oint_A \rho_1 \mathbf{v}_{li} \hat{n} dA = \int_{\Omega} \nabla \cdot (\rho_1 \mathbf{v}_{li}) d\Omega \quad (21)$$

Substitution of Eq.(21) into Eq.(20) results in

$$\int_{\Omega} \left\{ \frac{\partial[\rho_1(1+e)n_1]}{(1+e)\partial t} + \nabla \cdot (\rho_1 \mathbf{v}_{li}) - \rho_1 q_1 \right\} d\Omega = 0 \quad (22)$$

The unit body Ω is chosen at random. So as long as the integrand is continuous, the entire integral over the body is equal to 0, which in turn requires that its integrand must be 0. Therefore, the differential governing equation for water flow is

$$\frac{\partial[\rho_1(1+e)n_1]}{(1+e)\partial t} + \nabla \cdot (\rho_1 \mathbf{v}_{li}) = \rho_1 q_1 \quad (23)$$

Expanding the left-hand side of Eq.(23) and introducing Eq.(14) results in

$$\rho_1 n_1 \frac{\partial \varepsilon_v}{\partial t} + \rho_1 \frac{\partial n_1}{\partial t} + n_1 \frac{\partial \rho_1}{\partial t} + \nabla \cdot \left[-\frac{\rho_1 \mathbf{k}_{lij}}{\mu_1} \left(\frac{\partial p_i}{\partial x_j} + \rho_1 g_j \right) - \rho_1 \mathbf{k}_{lrij} \frac{\partial T}{\partial x_j} \right] = \rho_1 q_1 \quad (24)$$

According to Eq.(6), the changing rate of liquid water content can be expressed as

$$\frac{\partial n_1}{\partial t} = B'_3 \frac{\partial \varepsilon_v}{\partial t} + B'_4 \frac{\partial p_c}{\partial t} + B'_5 \frac{\partial T}{\partial t} \quad (25)$$

The change of liquid water density due to temperature and water pressure variations can be derived from the equation of state for water, given by Zhou [28] as

$$\rho_1 = \rho_{10} \{1 + \beta_1[(p_c + p_a) - (p_{c0} + p_{a0})] - \alpha_1(T - T_0)\} \quad (26)$$

where ρ_{10} is the initial density of water, α_1 is the thermal expansion coefficient and β_1 is the compressibility.

Substitution of Eqs.(25) and (26) into Eq.(24) results in

$$L_{11} \frac{\partial \varepsilon_v}{\partial t} + L_{12} \frac{\partial p_c}{\partial t} + L_{13} \frac{\partial p_a}{\partial t} + L_{14} \frac{\partial T}{\partial t} + \nabla \cdot \left[-\frac{\rho_1 \mathbf{k}_{lij}}{\mu_1} \left(\frac{\partial p_i}{\partial x_j} + \rho_1 g_j \right) - \rho_1 \mathbf{k}_{lrij} \frac{\partial T}{\partial x_j} \right] = \rho_1 q_1 \quad (27)$$

where $L_{11} = \rho_1(n_1 + B'_3)$, $L_{12} = \rho_1 B'_4 + \rho_{10} \beta_1 n_1$, $L_{13} = \rho_{10} \beta_1 n_1$, and $L_{14} = \rho_1 B'_5 - \rho_{10} \alpha_1 n_1$.

2.3.3 Air mass conservation equation

Neglecting the inertial and viscous effects, the equation of linear momentum balance for the air can be written as

$$\mathbf{v}_{ai} = -\frac{\mathbf{k}_{aij}}{\mu_a} \frac{\partial p_a}{\partial x_j} - \mathbf{k}_{aTij} \frac{\partial T}{\partial x_j} \quad (28)$$

where \mathbf{k}_{aTij} is a tensor representing the effects of thermal coupling for air; μ_a is the dynamic viscosity of air; and \mathbf{k}_{aij} is the permeability tensor of air, which is often written as

$$\mathbf{k}_{aij} = \mathbf{k}_{ij} k_a^r \quad (29)$$

where k_a^r is the relative permeability of air.

Similar to the derivation process for water, the differential governing equation for air flow is

$$\frac{\partial[\rho_a(1+e)n_a]}{(1+e)\partial t} + \nabla \cdot (\rho_a \mathbf{v}_{ai}) = \rho_a q_a \quad (30)$$

Expanding the left-hand side of Eq.(28) leads to

$$\begin{aligned} \frac{\partial[\rho_a(1+e)n_a]}{(1+e)\partial t} &= \frac{\partial\{\rho_a[e - (1+e)n_1]\}}{(1+e)\partial t} = \\ &= \frac{\partial\rho_a e}{(1+e)\partial t} - \frac{\partial[\rho_a(1+e)n_1]}{(1+e)\partial t} \end{aligned} \quad (31)$$

Regarding air as an ideal gas, its equation of state is given by

$$\rho_a = \frac{p_a}{RT} \quad (32)$$

where R is the specific gas constant.

Substitution of Eqs.(6), (31) and (32) into Eq.(30) results in the following air conservation equation:

$$\begin{aligned} L_{21} \frac{\partial \varepsilon_v}{\partial t} + L_{22} \frac{\partial p_c}{\partial t} + L_{23} \frac{\partial p_a}{\partial t} + L_{24} \frac{\partial T}{\partial t} + \\ \nabla \cdot \left(-\frac{p_a \mathbf{k}_{aij}}{\mu_a} \frac{\partial p_a}{\partial x_j} - \rho_a \mathbf{k}_{aTij} \frac{\partial T}{\partial x_j} \right) = \rho_a q_a \end{aligned} \quad (33)$$

where $L_{21} = \rho_a(1 - n_l - B'_3)$, $L_{22} = -\rho_a B'_4$, $L_{23} = \frac{n_a}{R(T + T_0)}$, and $L_{24} = -\left[\frac{n_a p_a}{R(T + T_0)^2} + \rho_a B'_5 \right]$.

2.3.4 Energy conservation equation

(1) Heat conservation equation for solid phase

Choosing a random unit body of volume Ω with an external surface area A and an exterior normal direction \hat{n} as defined before, the thermal energy increment per unit time by heat flow from an external source (for example, steam injection or electric heating) is

$$-\int_A \hat{Q} \hat{n} dA = -\int_{\Omega} \nabla \cdot \mathbf{Q} d\Omega = \int_{\Omega} \nabla \cdot (\lambda_{sij} \nabla T) d\Omega \quad (34)$$

where λ_{sij} is the thermal conductivity of solids.

The increase of heat energy Q_s caused by an internal heat source is

$$H_1 = \int_{\Omega} Q_s d\Omega \quad (35)$$

It is assumed that the density and specific heat of solid grains are ρ_s and c_s , respectively. If the temperature of the unit volume is increased by T , the needed heat energy is $\rho_s c_s T$, and the rate of change is $\partial(\rho_s c_s T) / \partial t$, therefore, the integral form of the energy equation for the solids is

$$\int_{\Omega} \left[\frac{\partial}{\partial t} (\rho_s c_s T) - \nabla \cdot (\lambda_{sij} \nabla T) - Q_s \right] d\Omega = 0 \quad (36)$$

As mentioned earlier, the energy balance equation for the solid phase can be written as

$$\frac{\partial}{\partial t} (\rho_s c_s T) = \nabla \cdot (\lambda_{sij} \nabla T) + Q_s \quad (37)$$

(2) Heat conservation equation for water (liquid phase)

The heat conservation equation for water can be obtained based on a Lagrangian description. For a certain material system where neither internal energy nor mechanical energy flows into or out from it, the material derivative of the sum of the heat energy needed by the increment of temperature is equal to that of the mechanical energy and the source term, which can be expressed by

$$\int_{\Omega} \left[\frac{d}{dt} (\rho_c T)_l - \nabla \cdot (\lambda_{lij} \nabla T) - Q_l \right] d\Omega = 0 \quad (38)$$

where c_l and T_l are the density, specific heat and temperature of the water, respectively; λ_{lij} is the thermal conductivity of water; and Q_l is the heat source of water.

As described above, the volume Ω is selected randomly, and the expression within the entire square bracket in Eq.(38) equals 0. Using the material derivative expression:

$$\frac{dF}{dt} = \frac{\partial F}{\partial t} + (\mathbf{v} \cdot \nabla) F \quad (39)$$

the energy balance equation for water can be written as

$$\frac{\partial}{\partial t} (\rho_c T)_l + (\mathbf{v}_l \cdot \nabla) (\rho_c T)_l = \nabla \cdot (\lambda_{lij} \nabla T) + Q_l \quad (40)$$

(3) Heat conservation equation for air (gas phase)

The heat energy conservation equation for air is similar to the one for water, and is expressed as

$$\frac{\partial}{\partial t} (\rho_a T)_a + (\mathbf{v}_a \cdot \nabla) (\rho_a T)_a = \nabla \cdot (\lambda_{aij} \nabla T) + Q_a \quad (41)$$

where ρ_a , c_a and T_a are the density, specific heat and temperature of air, respectively; λ_{aij} is the thermal conductivity of air; and Q_a is the heat source of air.

(4) The total heat energy conservation equation

The energy balance equations for solid, liquid (water) and air (gas) phases are derived separately above. These three equations need to be combined to establish a unified energy conservation equation for a porous medium under non-isothermal and unsaturated conditions. Assuming that the specific heat capacity and thermal conductivity λ are constant, and considering that the volumes of the solid, fluid and air phases occupied in the unit volume Ω are $1/(1+e)$, n_1 and $e/(1+e) - n_1$, respectively, the general energy conservation equation can be represented as

$$\begin{aligned} & \frac{\partial}{(1+e)\partial t} \{(\rho c T)_s + (1+e)n_1(\rho c T)_l + [e - (1+e)n_1] \cdot \\ & (\rho c T)_a\} + [(\mathbf{v}_l \cdot \nabla)(\rho c T)_l + (\mathbf{v}_a \cdot \nabla)(\rho c T)_a] = \\ & \nabla \cdot \left\{ \left[\frac{1}{1+e} \lambda_{sij} + n_1 \lambda_{lij} + \frac{e - (1+e)n_1}{1+e} \lambda_{aij} \right] \nabla T \right\} + \\ & \frac{1}{1+e} Q_s + n_1 Q_l + \frac{e - (1+e)n_1}{1+e} Q_a \end{aligned} \quad (42)$$

Coexisting water, air and solid components are assumed to be in local thermal equilibrium (i.e. locally they are at the same temperature). Reorganizing the above equations, the following equations can be obtained:

$$\begin{aligned} & L_{31} \frac{\partial \varepsilon_v}{\partial t} + L_{32} \frac{\partial p_c}{\partial t} + L_{33} \frac{\partial p_a}{\partial t} + L_{34} \frac{\partial T}{\partial t} + \\ & [(\mathbf{v}_l \cdot \nabla)(\rho c T)_l + (\mathbf{v}_a \cdot \nabla)(\rho c T)_a] = \\ & \nabla \cdot \left\{ \left[\frac{1}{1+e} \lambda_{sij} + n_1 \lambda_{lij} + \frac{e - (1+e)n_1}{1+e} \lambda_{aij} \right] \nabla T \right\} + \\ & \frac{1}{1+e} Q_s + n_1 Q_l + \frac{e - (1+e)n_1}{1+e} Q_a \end{aligned} \quad (43)$$

where $L_{31} = (c_l L_{11} + c_a L_{21})T$, $L_{32} = (c_l L_{12} + c_a L_{22})T$,
 $L_{33} = (c_l L_{13} + c_a L_{23})T$, $L_{34} = (\rho c)_m^* + (c_l L_{14} + c_a L_{24})T$,
and $(\rho c)_m^* = \frac{\rho_s c_s + \rho_l c_l (1+e)n_1 + \rho_a c_a [e - (1+e)n_1]}{1+e}$.

3 Numerical solution

Equations (13), (27), (33) and (43) represent the governing equations for the coupled thermo-hydro-mechanical model of unsaturated porous media. They are solved numerically by a finite element method based on the Galerkin formulation. The program flowchart is illustrated in Fig.1. The following assumptions are made for numerical analysis. (1) The Drucker-Prager criterion is used to define yield locus and plastic potential. (2) The associated flow rule and Generalized Newton-Raphson

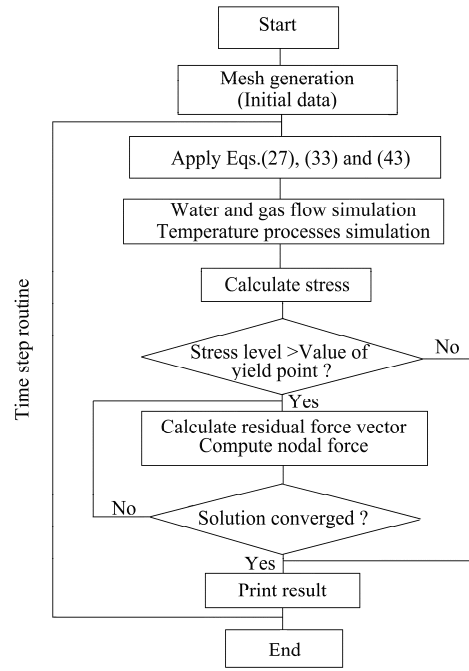


Fig.1 Program flowchart.

method are used to solve the nonlinear equations.

4 Engineering application of model

4.1 Numerical model and parameters

As an example of the coupled THM response for a practical engineering setting, take a hypothetical underground horizontal tunnel in argillite rock that is 5.9 m in diameter and 500 m below the ground surface. A numerical simulation is conducted to explain unsaturated water flow, temperature and mechanical behavior of the argillite during shaft excavation, ventilation and concrete lining stages. The thickness of concrete lining is 0.45 m. Figure 2 shows a schematic diagram of the numerical model and its boundary conditions.

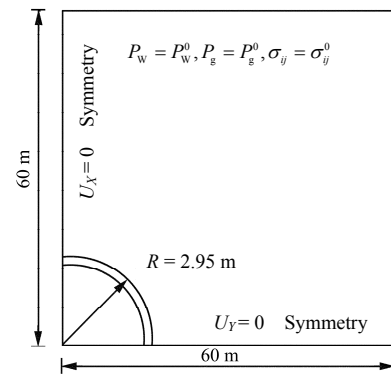


Fig.2 2D finite element model and boundary conditions.

Since the shaft is located 500 m underground, it was assumed that before shaft excavation, the pore-water pressure and the pore-air pressure in the argillite were

both 4 MPa and that the temperature in the surrounding argillite was 293.15 K. After shaft excavation, the pore-water pressure and the pore-air pressure were −38.4 and 0.1 MPa, respectively, due to shaft ventilation. For the precast concrete linings, the initial pore-water pressure and pore-air pressure were assumed to be −14.4 and 0.1 MPa, respectively. The concrete lining was assumed to have been installed 8 days after the shaft excavation. After the concrete lining was installed, the pore-water pressure and the pore-air pressure on the internal surface of the concrete lining were also assumed to be −14.4 and 0.1 MPa, respectively. A steady heat source with a constant temperature $T = 353.15$ K at the internal boundary of tunnel was maintained for one year.

For the in-situ stress field, it was assumed that the vertical stress $\sigma_z = 12.0$ MPa, with a linear variation coefficient $K = \sigma_H / \sigma_z$ for the horizontal stress component. Relationships suggested for the calculation of saturation degree, relative water permeability and relative gas permeability of argillite and concrete are shown in Table 1 [29]. The 2D finite element model and boundary conditions are shown in Fig.2. The hydraulic, thermal and mechanical parameters of argillite and concrete are shown in Tables 2 and 3 [30, 31].

Table 1 Relationship of the relative permeability of water and gas in argillite and concrete with saturation degree [29].

Material	Relationship between saturation degree and capillary pressure	Relationship between saturation degree and relative water permeability	Relationship between saturation degree and relative air permeability
Argillite	$S_w = \frac{a}{a + (p_c / 10\,000)^b}$ $a = 2\,846, b = 0.906$	$k_{r1} = \frac{1}{1 + [a(1 - S_w)]^b}$ $a = 35, b = 1.5$	$k_{r2} = \frac{1}{1 + (aS_w)^b}$ $a = 3, b = 2.7$
Concrete	$S_w = [1 + (ap_c)^b]^c$ $a = 2.35 \times 10^{-8}, b = 1.827, c = -0.577$	$k_{r1} = S_w^{1/2} [1 - (1 - S_w^{1/d})^2]^2$ $d = 0.435\,991$	$k_{r2} = \sqrt{1 - S_w} (1 - S_w^{1/d})^{2d}$ $d = 0.435\,991$

Table 2 Hydro-thermal parameters of argillite and concrete [30, 31].

Material	Initial density (kg/m ³)	Intrinsic permeability (m ²)	Initial porosity	Dynamic viscosity	Specific heat capacity (J/(kg·°C))	Thermal conductivity (W/(m·°C))
Argillite	2 500	1×10^{-19}	0.14	—	837	2.5
Concret	2 600	1×10^{-18}	0.16	—	993	2.2
Water	1 000	—	—	Eq.(16)	4 186	0.56
Air	Eq.(32)	—	—	1.846×10^{-7}	1 000	0.30

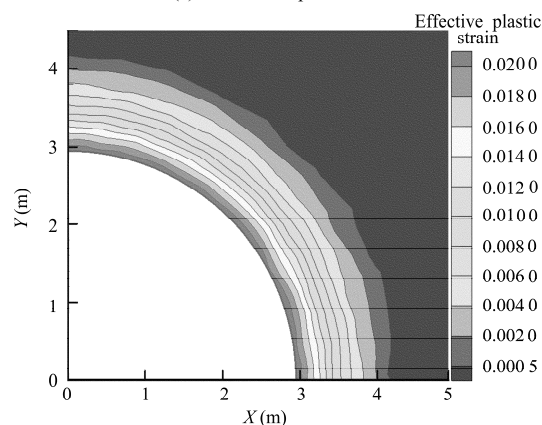
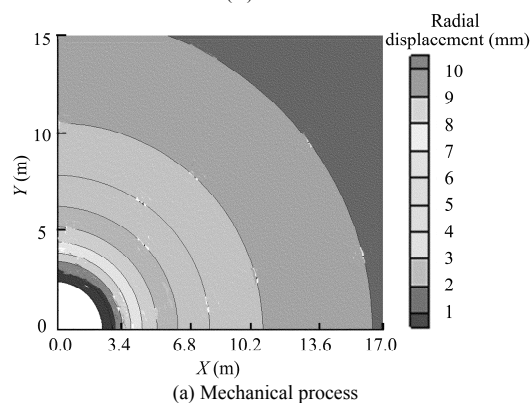
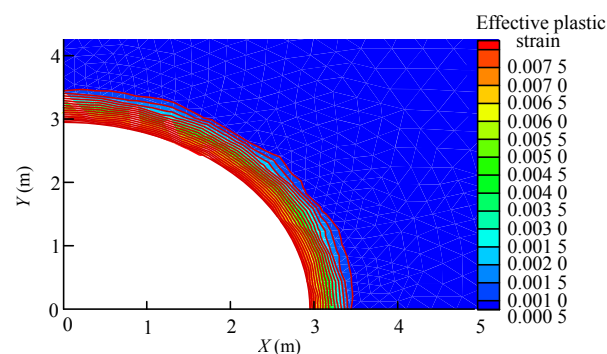
Table 3 Mechanical parameters of argillite and concrete [30, 31].

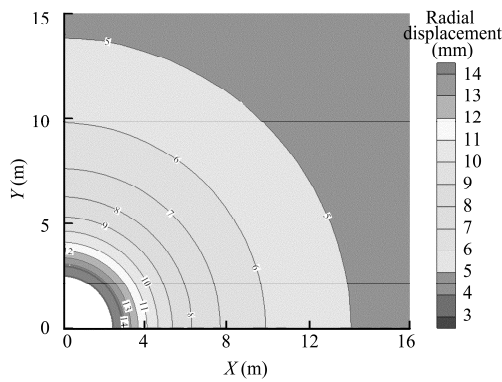
Material	Young's modulus (GPa)	Poisson's ratio	Cohesion (MPa)	Friction angle (°)	Thermal expansion coefficient
Argillite	3.8	0.30	8.8	20	1.0×10^{-5}
Concrete	10.0	0.17	—	—	1.0×10^{-5}

4.2 Numerical results

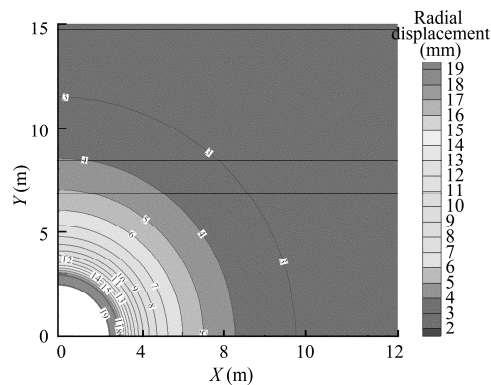
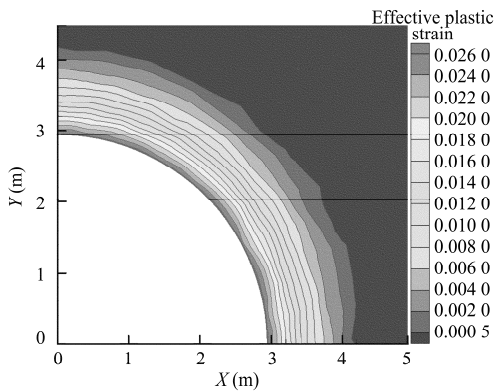
The main objective of our research was to study the coupled THM behavior of argillite while considering the influences of: (1) temperature on the dynamic viscosity of liquid water and void ratio, (2) liquid flow on temperature (thermo-osmosis), (3) deformability on mass and heat conservation equations, and (4) heat flow on water potential gradient.

First, to illustrate the necessity of coupled analysis, three results are shown for: (1) the effective plastic strain and the radial displacement of the shaft considering only the mechanical process (Fig.3(a)), (2) the coupled hydro-mechanical processes (Fig.3(b)), and (3) the coupled THM processes (Fig.3(c)). As expected, the maximum effective plastic strains are 0.007 5, 0.02, and 0.026, and the maximum radial displacements are 10, 14, and 19 mm, respectively. The comparison indicates capillary pressure and temperature both have a strong influence on the mechanical properties.





(b) Hydro-mechanical process



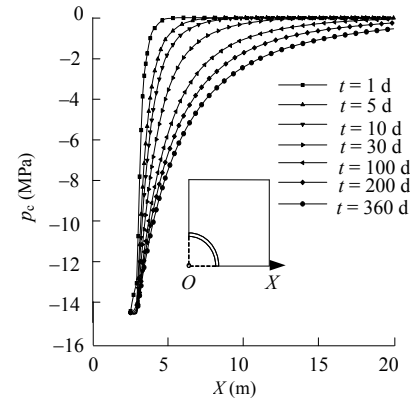
(c) Thermo-hydro-mechanical process

Fig.3 Distributions of effective plastic strain and radial stress.

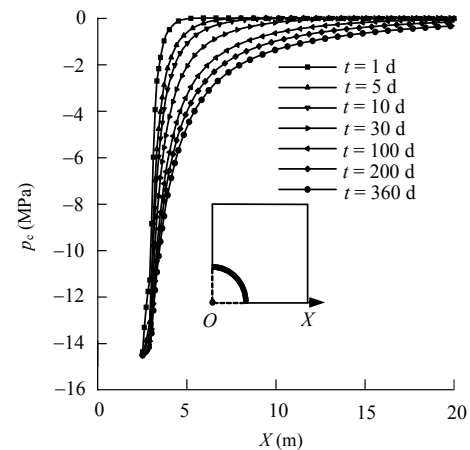
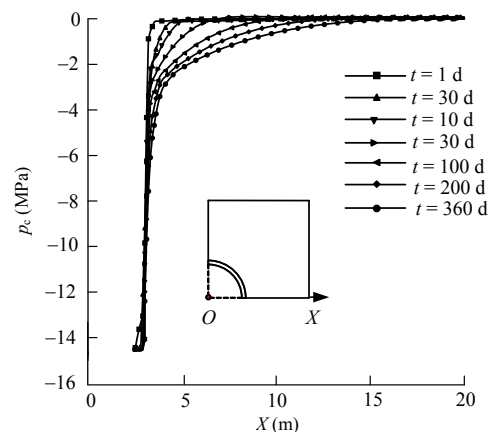
Second, to examine the influence of liquid flow due to thermal gradients and deformation, analyses were conducted under the following conditions:

(1) $D_T = 0$, and the effect of the volumetric strain on water and air flow and heat transfer processes are considered. A comparison of Figs.4(a) and (b) indicates that the coefficient D_T has a significant effect on capillary pressure.

(2) $D_T = 0$, and the effects of solid deformability on water and air mass flow and heat transfer processes are neglected. Figure 4(c) shows that increases of capillary pressure are overestimated if the effects of solid deformability are neglected. The larger increase of capillary pressure in Figs.4(a) and (b) is due to the rigidity of the medium.



(a) Capillary pressure distribution.

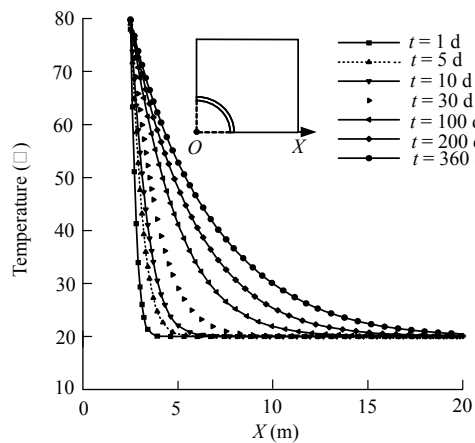
(b) Capillary pressure distribution ($D_T = 0$).(c) Capillary pressure distribution ($D_T = 0$, and neglecting the effects of deformability).**Fig.4** Capillary pressure distributions.

Finally, to evaluate the influence of temperature distribution due to water flow (convection) and deformation, analyses are considered under the following conditions:

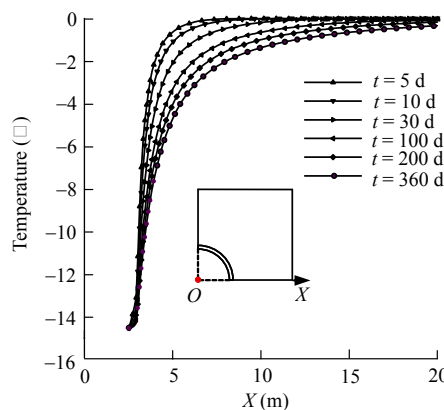
(1) Neglecting thermal convection (by water flow), but considering the effect of volumetric strain on fluid flow and heat transfer equations. A comparison of Figs.5(a) and (b) indicates that the temperature becomes stable more quickly when considering the effects of thermal convection. This is because the

directions of water flow and thermal transmission are opposite.

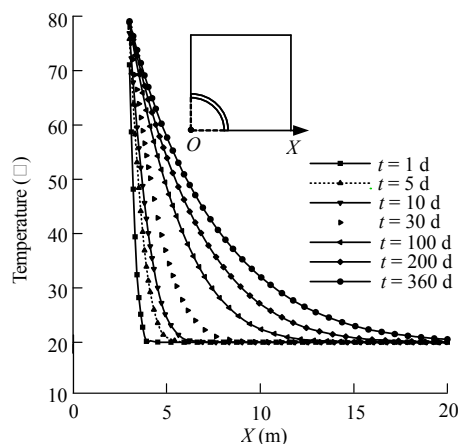
(2) Neglecting the thermal convection (by water flow) and the effects of deformation on water and air flows and heat transfer processes. Figure 5(c) shows that the time needed to stabilize temperature is shorter than that shown in Fig.5(b), which means that it is not accurate without considering the effects of deformation to simulate the temperature distribution.



(a) Temperature distribution along X axis.



(b) Temperature distribution along X axis without considering water flow (convection).



(c) Temperature distribution along X axis without considering water flow and the effects of deformability (convection).

Fig.5 Temperature distribution.

5 Conclusions

The main objectives of this study were to derive a fully coupled THM model for unsaturated argillite and to simulate the evolution of unsaturated water flow in a hypothetical (but logistically reasonable) tunnel through such an argillite during excavation, ventilation and concrete lining stages. A fully coupled THM model for unsaturated argillite is presented to simulate the complex coupling problems. The model consists of the equilibrium equation and the conservation equations for mass and energy. The coupling process takes into account: (1) the effect of temperature on the dynamic viscosity of liquid water and void ratio, (2) the influence of liquid flow on temperature gradient, (3) effects on water flow, and (4) the influence of heat flow due to thermal convection. Numerical results show that: (1) the consideration of deformation in mass and heat balance equations and (2) fully coupled heat-water flow ($D_T \neq 0$) can result in substantially different solutions. Therefore, the novel fully coupled model can be useful for petroleum engineering, underground disposal of nuclear waste, geothermal energy development, construction in cold regions and numerous other applications. The formulation, however, does not consider mass transfer in liquid and gas phases. Thus, a theoretical coupled model that incorporates gaseous flow would be a suitable subject of future research.

References

- [1] Detournay E, Cheng A H D. Poroelastic response of a borehole in a non-hydrostatic stress field. *International Journal of Rock Mechanics and Mining Sciences and Geomechanics Abstracts*, 1988, 25 (3): 171–182.
- [2] Cheng A H D, Abousleiman Y, Roegiers J C. Review of some poroelastic effects in rock mechanics. *International Journal of Rock Mechanics and Mining Sciences and Geomechanics Abstracts*, 1993, 30 (7): 1 119–1 126.
- [3] Senjuntichai T. Green's functions for multi-layered poroelastic media and an indirect boundary element method. PhD Thesis. Winnipeg: University of Manitoba, 1994.
- [4] McTigue D. Thermoelastic response of fluid-saturated porous rock. *Journal of Geophysical Research*, 1986, 91 (B9): 9 533–9 542.
- [5] Smith D, Booker J. Green's functions for a fully coupled thermoporoelastic material. *International Journal for Numerical and Analytical Methods in Geomechanics*, 1993, 30 (6): 354–355.
- [6] Jiang Q, Rajapakse R K N D. On coupled heat-moisture transfer in deformable porous media. *Quarterly Journal of Mechanics and Applied Mathematics*, 1994, 47 (1): 53–68.

- [7] Wang Y, Papamichos E. Conductive heat flow and thermal induced fluid flow around a well bore in a poroelastic medium. *Water Research*, 1994, 30 (12): 3 375–3 384.
- [8] Rehbinder G. Analytical solutions of stationary coupled thermo-hydro-mechanical problems. *International Journal of Rock Mechanics and Mining Sciences and Geomechanics Abstracts*, 1995, 32 (5): 453–463.
- [9] Lewis R W, Schrefler B A. The finite element method in the deformation and consolidation of porous media. New York: Wiley, 1987.
- [10] Britto A M, Savvidou C, Gunn M J, et al. Finite element analysis of the coupled heat flow and consolidation around hot buried objects. *Soils and Foundations*, 1992, 32 (1): 13–25.
- [11] Kim J M, Parizek R R. Three-dimensional finite element modelling for consolidation due to groundwater withdrawal in a desaturating anisotropic aquifer system. *International Journal for Numerical and Analytical Methods in Geomechanics*, 1999, 23 (6): 549–571.
- [12] Alonso E E, Gens A, Josa A A. A constitutive model for partially saturated soils. *Géotechnique*, 1990, 40 (3): 405–430.
- [13] Alonso E E, Vaunat J, Gens A. Modelling the mechanical behaviour of expansive argillites. *Engineering Geology*, 1999, 54 (1/2): 173–183.
- [14] Maatouk A, Leroueil S, La Rochelle P. Yielding and critical state of a collapsible unsaturated silty soil. *Géotechnique*, 1995, 45 (3): 435–477.
- [15] Schmitt L, Forsans T, Santarelli F J. Shale testing and capillary phenomena. *International Journal of Rock Mechanics and Mining Sciences and Geomechanics Abstracts*, 1994, 31 (5): 411–427.
- [16] Armero F. Formulation and finite element implementation of a multiplicative model of coupled poro-plasticity at finite strains under fully saturated conditions. *Computer Methods in Applied Mechanics and Engineering*, 1999, 171 (3/4): 205–241.
- [17] Borja R I, Alarc E. A mathematical framework for finite strain elastoplastic consolidation. part 1: balance laws variational formulation, and linearization. *Computer Methods in Applied Mechanics and Engineering*, 1995, 122 (1/2): 145–171.
- [18] Diebels S, Ehlers W. Dynamic analysis of a fully saturated porous medium accounting for geometrical and material nonlinearities. *International Journal for Numerical and Analytical Methods in Geomechanics*, 1996, 39: 81–97.
- [19] Wilmanski K. Porous medium at finite strains-the new model with the balance equation for porosity. *Arch. Mech.*, 1996, 48 (4): 591–628.
- [20] Kempa W. On the description of the consolidation phenomenon by means of a two-component continuum. *Archives of Mechanics*, 1997, 49 (5): 893–917.
- [21] Noorishad J, Tsang C F, Witherspoon P A. Coupled thermal-hydraulic-mechanical phenomena in saturated fractured porous rocks: Numerical approach. *Journal of Geophysical Research*, 1984, 89 (12): 10 365–10 373.
- [22] Hudson J A, Stephansson O, Andersson J, et al. Coupled T-H-M issues relating to radioactive waste repository design and performance. *International Journal of Rock Mechanics and Mining Sciences*, 2001, 38 (1): 143–161.
- [23] Rutqvist J, Borgesson L, Chijimatsu M, et al. Thermohydromechanics of partially saturated geological media: governing equations and formulation of four finite element models. *International Journal of Rock Mechanics and Mining Sciences*, 2001, 38 (1): 105–127.
- [24] McDougall J R, Sarsby R W, Hill H J. A numerical investigation of landfill hydraulics using variably saturated flow theory. *Géotechnique*, 1996, 46 (2): 329–341.
- [25] Wan A W L. The use of thermocouple psychrometers to measure in situ suctions and water contents in compacted argillites. PhD Thesis. Winnipeg: University of Manitoba, 1996.
- [26] Wheeler S J, Sivakumar V. Development and application of a critical state model for unsaturated soil. In: *Predictive Soil Mechanics, Proceedings of the Wroth Memorial Symposium*. London: Thomas Telford, 1993: 709–728.
- [27] Fredlund D G, Rachardjo E. Soil mechanics for unsaturated soils. New York: Wiley, 1993.
- [28] Zhou Y F. Thermo-hydro-mechanical models for saturated and unsaturated porous media. PhD Thesis. Winnipeg: University of Manitoba, 1998.
- [29] Chen W Z, Shao J F, Duveau G, et al. Constitutive model of saturated-unsaturated argillite and its numerical simulation. *Chinese Journal of Rock Mechanics and Engineering*, 2005, 24 (17): 13–18 (in Chinese).
- [30] Chen W Z, Shao J F, Yang C H, et al. Research on saturated and unsaturated flow mechanism of argillite. *Chinese Journal of Rock Mechanics and Engineering*, 2004, 24 (21): 128–133 (in Chinese).
- [31] Shao J F, Duveau G, Bourgeois F, et al. Elastoplastic damage modeling in unsaturated rocks and applications. *International Journal of Geomechanics*, 2006, 6 (2): 119–130.